https://doi.org/10.5194/acp-2021-405
Preprint. Discussion started: 19 May 2021

Atmospheric Chemistry and Physics Discussions

Heterogeneity and Chemical Reactivity of the Remote Troposphere defined by Aircraft Measurements

Hao Guo[1], Clare M. Flynn[2], Michael J. Prather[1], Sarah A. Strode[3], Stephen D. Steenrod[3], Louisa Emmons[4], Forrest Lacey[4,5], Jean-Francois Lamarque[4], Arlene M. Fiore[6], Gus Correa[6], Lee T. Murray[7], Glenn M. Wolfe[3,8], Jason M. St. Clair[3,8], Michelle Kim[9], John Crounse[10], Glenn Diskin[10], Joshua DiGangi[10], Bruce C. Daube[11,12], Roisin Commane[11,12], Kathryn McKain[13,14], Jeff Peischl[14,15], Thomas B. Ryerson[13,15], Chelsea Thompson[13], Thomas F. Hanisco[3], Donald Blake[16], Nicola J. Blake[16], Eric C. Apel[4], Rebecca S. Hornbrook[4], James W. Elkins[14], Eric J. Hintsa[13,14], Fred L. Moore[13,14], Steven Wofsy[11]

[1] Department of Earth System Science, University of California, Irvine, CA 92697
[2] Department of Meteorology, Stockholm University, Stockholm SE-106 91, Sweden
[3] Atmospheric Chemistry and Dynamics Laboratory, NASA Goddard Space Flight Center, Greenbelt, MD 20771
[4] Atmospheric Chemistry Observations and Modeling Laboratory, National Center for Atmospheric Research, Boulder, CO 80301
[5] Department of Mechanical Engineering, University of Colorado, Boulder, CO 80309
[6] Department of Earth and Environmental Sciences and Lamont-Doherty Earth Observatory, Columbia University, Palisades, NY 10964
[7] Department of Earth and Environmental Sciences, University of Rochester, Rochester, NY 14611
[8] Joint Center for Earth Systems Technology, University of Maryland, Baltimore County, Baltimore, MD 21228
[9] Department of Geological and Planetary Sciences, California Institute of Technology, Pasadena, CA 91125
[10] Atmospheric Composition, NASA Langley Research Center, Hampton VA 23666
[11] John A. Paulson School of Engineering and Applied Sciences, Harvard University, Cambridge, MA 02138
[12] Department of Earth and Planetary Sciences, Harvard University, Cambridge, MA 02138
[13] Cooperative Institute for Research in Environmental Sciences, University of Colorado, Boulder, CO 80309
[14] Global Monitoring Division, Earth System Research Laboratory, NOAA, Boulder, CO 80305
[15] Chemical Sciences Division, National Oceanic and Atmospheric Administration Earth System Research Laboratory, Boulder, CO 80305
[16] Department of Chemistry, University of California, Irvine, CA 92697

Correspondence to: Hao Guo (haog2@uci.edu) and Michael J. Prather (mprather@uci.edu).

Keywords: Tropospheric Chemistry, Ozone, Methane, Aircraft Observations, NASA ATom

https://doi.org/10.5194/acp-2021-405
Preprint. Discussion started: 19 May 2021

Atmospheric Chemistry and Physics Discussions

Abstract

The NASA Atmospheric Tomography (ATom) mission built a photochemical climatology of air parcels based on in situ measurements with the NASA DC-8 aircraft along objectively planned profiling transects through the middle of the Pacific and Atlantic Oceans. ATom measured numerous gases and aerosols, particularly the gaseous species driving the chemical budgets of O_3 and CH_4: i.e., O_3, CH_4, CO, C_2H_6, higher alkanes, alkenes, aromatics, NO_x, HNO_3, HNO_4, peroxyacetylnitrate, other organic nitrates, H_2O, HCHO, H_2O_2, and CH_3OOH. From the 10 s (2 km) merged observations, a modeling data stream (MDS) based on observations of the core species, consisting of 146,494 distinct air parcels has been constructed from the 4 ATom deployments, providing a continuous data stream for initializing global chemistry models and calculating the 24-hour chemical tendencies. Tendencies derived from 6 chemistry models using the ATom-1 MDS tend to agree and show a highly heterogeneous troposphere where globally 10% of the parcels control as much as 40% of the budget of O_3 and CH_4. Surprisingly, modeled probability distributions (100-km cells) match ATom statistics (2 km parcels), indicating that the majority of the observed heterogeneity can be resolved with current global chemistry models. On the other hand, the models' own chemical climatologies underestimate O_3 production below 4 km in both Pacific and Atlantic basins because they have lower NO_X levels than observed.

1.Introduction

The NASA Atmospheric Tomography (ATom) mission completed a four-season deployment. Each deployment flying from the Arctic to Antarctic and back, traveling south through the middle of the Pacific Ocean, across the Southern Ocean, and then north through the Atlantic Ocean, with near-constant profiling of the marine troposphere from 0.2 to 12 km altitude (See Figure S1). The DC8 was equipped with in situ instruments that documented the chemical composition and conditions at time intervals ranging from <1 to about 100 seconds (Wofsy et al., 2018). ATom measured hundreds of gases and aerosols, providing information on the chemical patterns and reactivity in the vast remote ocean basins, where most of the destruction of tropospheric ozone (O_3) and methane (CH_4) occurs. Reactivity is defined here as in Prather et al. (2017) to include the production and loss of O_3 (P-O3 and L-O3, ppb/d) and loss of CH_4 (L-CH4, ppb/d). Here we report on this model-derived product that was proposed for ATom, the daily averaged reaction rates determining the production and loss of O_3 and loss of CH_4 for 10 s averaged air parcels. We calculate these rates with 3D chemical models that include variations in clouds and photolysis, and then assemble the statistical patterns describing the heterogeneity (i.e., high spatial variability) of these rates and the underlying patterns of reactive gases that are responsible for the net reactivity.

Tropospheric O_3 and CH_4 contribute to climate warming and global air pollution (Stocker et al, 2013). Their abundances in the troposphere are controlled largely by tropospheric chemical reactions. Thus, chemistry-climate assessments seeking to understand past global change and make future projections for these greenhouse gases have focused on the bulk tropospheric rates of production and loss, and how these reactivities are distributed in large zones throughout the troposphere (Griffiths et al., 2020; Myhre et al.,2013; Naik et al., 2013; Prather et al., 2001; Stevenson, et al., 2006; Stevenson, et al., 2013; Stevenson, et al., 2020; Voulgarakis et al., 2013; Young et al., 2013). The models used in these assessments disagree on these overall CH_4 and O_3 reactivities, and resolving the cause of such differences is stymied because of the large number of processes involved and the resulting highly heterogeneous distribution of chemical species that drive the reactions. Simply put, the models use emissions, photochemistry, and meteorological data to generate the distribution of key species such as nitrogen oxides (NO_x = NO + NO_2) and

https://doi.org/10.5194/acp-2021-405
Preprint. Discussion started: 19 May 2021


Atmospheric Chemistry and Physics Discussions

hydrogen peroxide (HOOH) (step 1) and then calculate the CH_4 and O_3 reactivities from these species (step 2). Stratospheric studies such as Douglass et al. (1999) have provided a quantitative basis for testing chemistry and transport, and defining model errors; but few of these studies have tackled the problem of modeling the heterogeneity of tropospheric chemistry. The major model differences lie in the first step, because when we specify the mix of key chemical species, most models agree on the CH_4 and O_3 chemical budgets (Prather et al., 2018). The intent of ATom was to collect an atmospheric sampling of all the key species, the statistics defining their spatial variability, and that of the reactivities of CH_4 and O_3.

Many studies have explored the ability of chemistry-transport models (CTMs) to resolve finer scales including pollution layers (Eastham et al., 2017; Rastigejev et al., 2010; Tie et al., 2010; Young et al., 2018; Zhuang et al., 2018), but these have not had the observations of chemical statistics to evaluate model performance. In a great example of using chemical statistics, Yu et al. (2016) used 60 s data (~12 km) from the SEAC^{4}RS aircraft mission to compare cumulative probability distribution functions of NOx, O_3, HCHO, and isoprene over the Southeast US with the GEOS-Chem CTM run at different resolutions. They identified clear biases at the high and low ends of the distribution, providing a new test of models based on the statistics rather than mean values. Heald et al. (2011) gathered high resolution profiling of organic and sulfate aerosols from 17 aircraft missions and calculated statistics (mean, median, quartiles) but only compared with the modeled means. The HIAPER Pole-to-Pole Observations (HIPPO) aircraft mission (Wofsy, 2011) was a precursor to ATom with regular profiling of the mid-Pacific including high frequency 10 s sampling that identified the small scales of variability throughout the troposphere. HIPPO measurements were limited in species, lacking O_3, NOx and many of the core species needed for reactivity calculations. ATom, with a full suite of reactive species and profiling through the Atlantic basin, provides a wealth of chemical statistics to challenge the global chemistry models.

Our task here is the assembly of the modeling data stream (MDS) that provides flight-wise continuous 10 s data (air parcels) for the key reactive species as described in Methods and Supplementary Information. The MDS is based on direct observations and interpolation methods to fill gaps. From the MDS we have six chemical models calculate the 24 h reactivities, producing a reactivity data stream (RDS) as described in Methods and Supplementary Information. In the Results section, we examine the statistics of reactivity over the Atlantic and Pacific Oceans, focusing on air parcels with high reactivity, for example, 10% of the parcels produce 24-35% of total reactivity. We compare these ATom-1 statistics, species and reactivities, with August climatologies from six global chemistry models. Overall, ATom-1 shows a more reactive tropical and mid-latitude summer troposphere than found in most models' climatologies due primarily to higher NOx levels. Conclusions and discussion of opportunities for the ATom MDS+RDS datasets are presented in the Discussion. ATom measurements should provide fundamental performance metrics for all global chemistry models, metrics that define the chemical statistics of the troposphere and address the cause of differences in the O_3 and CH_4 budgets currently seen across the models. Use of the ATom MDS+RDS can help us identify patterns in key species that must be matched to capture the reactive chemistry of the remote troposphere.

2. Models and data

2.1 The modeling data stream

https://doi.org/10.5194/acp-2021-405
Preprint. Discussion started: 19 May 2021


Atmospheric Chemistry and Physics Discussions

The ATom mission was designed to collect a multi-species, detailed chemical climatology that documents the spatial patterns of chemical heterogeneity throughout the remote troposphere. Supplemental Figure S1 maps the 48 research flights, and the Supplementary Information has tables summarizing each flight. We required a complete set of key species in each air parcel to initialize models to be able to calculate the CH_4 and O_3 reactivities. We choose the key reactive species (H_2O, O_3, CO, CH_4, NO_x, NO_xPSS, HNO_3, HNO_4, PAN, CH_2O, H_2O_2, CH_3OOH, acetone, acetaldehyde, C_2H_6, C_3H_8, i-C_4H_{10}, n-C_4H_{10}, alkanes, C_2H_4, alkenes, C_2H_2, C_5H_8, benzene, toluene, xylene, CH_3ONO_2, $C_2H_5ONO_2$, $RONO_2$, CH_3OH) and then add corollary species or other data indicative of industrial or biomass-burning pollution or atmospheric processing (HCN, CH_3CN, SF_6, relative humidity, aerosol surface area (4 modes), and cloud indicator). We choose 10 s averages for our air parcels as a compromise and because the 10 s merged data is a standard product (Wofsy et al., 2018). A few instruments measure at 1 s intervals, but the variability at this scale is not that different from 10 s averages (Figure S2). Throughout ATom, gaps occur in individual species on a range of times scales due to calibration cycles, sampling rates, and instrument malfunction. The creation of the MDS used a range of methods to fill these gaps and assigned a flag index to each species, allowing users to avoid parcels with less reliable methods, on a species-by-species basis. The approach to gap filling is described in detail in the Supplementary Information.

2.2 The reactivity data stream.

The concept of using an MDS to initialize 3D global chemistry models and calculate an RDS was developed in the pre-ATom methodology papers (Prather et al., 2017; Prather et al., 2018). In this paper, we use the 6 models for their August chemical statistics, and use 5 of them plus a box model to calculate the reactivities (i.e., chemical tendencies) from the ATom-1 MDS, see Table 1. Large model differences are clearly seen in the parcel-by-parcel root-mean-square (RMS) differences summed across the RDS_R0 parcels in Table 3. Even when models adopt standard kinetic rates and cross sections (i.e., Burkholder et al., 2015), the number of species and chemical mechanisms included, as well as the treatment of families of similar species or intermediate short-lived reaction products, varies across models. For example, UCI considers about 32 reactive gases, whereas GC and GMI have over 100, and F0AM typically runs with more than 600. The other major difference across models is photolysis, with models having different cloud data and different methods for calculating photolysis rates in cloudy atmospheres (Hall et al., 2018).

3. Results

In developing the MDS, we mapped higher- and lower-frequency measurements onto 10 s air parcels and then tested our gap-filling procedures, see Methods. Examination of higher-frequency 1 s data available for O_3 and H_2O shows that 10 s averaging preserves most of the heterogeneity (Figure S2). Overall we tested 3 successive MDS revisions designated R0, R1, and R2. MDS_R0 for ATom-1 was distributed to the full ATom science team, and we received the modeled RDS_R0 from 5 of the original 6 global models (Prather et al., 2017) plus 1 box model, see Table 1. Three central models (GC, GMI, UCI) showed excellent agreement. The MDS_R1 release corrected the primary mistake in creating MDS_R0 (i.e., use of photostationary NOx instead of observed NOx) and was re-run with two models (GMI, UCI), again showing excellent agreement. MDS_R2 optimized and tested the treatments of gap filling and lower limit of detection, along with other quality controls. Because of previous model agreement and the relatively small changes from R1 to R2, we calculated RDS_R2 only with one model (UCI). The R1 and R2 NOx values are 25% larger on average than the R0 values (unweighted mean of 66 vs. 52 ppt), and this affects primarily P-O3 and secondarily L-CH4. For UCI, the RDS_R1 and RDS_R2 differences are very small and so we show here: RDS_R0 for all 6 models, RDS_R1 for

https://doi.org/10.5194/acp-2021-405
Preprint. Discussion started: 19 May 2021


Atmospheric Chemistry and Physics Discussions

GMI, and RDS_R2 for UCI as our best estimate. The MDS_R2 (and higher revisions) for ATom-2/3/4 are now public (https://espo.nasa.gov/atom/content/ATom); and while their RDS files are posted in the archive, the reactivities are not analyzed.

The reactivities for 3 large domains (Global, Pacific, Atlantic) from the 6 models' RDS_R0 are summarized in Tables 2 and S8. In our analysis, the ATom 10 s parcels are weighted to achieve uniform sampling from 200-1000 hPa and by cosine of latitude. Global reactivities are less than those of the ocean basins because they include high-latitude observations over the Southern Ocean and the Arctic. We include the statistics from UCI using alternate years (1997 and 2015 versus the standard 2016) to show the effect of different cloud fields, and also from the GMI RDS_R1 and UCI RDS_R2. The statistical properties of the reactivities include: mean value; percent of total reactivity in the top 10% parcels (Table 2); median; mean value of top 10% parcels; percent of total reactivity in the top 50% and top 3% parcels; mean photolysis rates (Table S8). These high-R parcels (3%, 10% and 50%) are determined separately for each model, each reactivity (R), and each domain.

The Atlantic is more reactive on average than the Pacific for all 3 Rs (P-O3, L-O3, L-CH4); however, the Pacific has a much more peaked high-R distribution as seen by the much higher fraction of the total contained in the top 10% (27-36% vs. 19-28%). The average R in the top 10% of parcels is typical 4 to 10 times the mean value; except again for Atlantic P-O3 for which it is only about 2.5 times higher. The key photolysis rates are similar across all models except GISS, and because of this and other inexplicable results, we drop these GISS R0 simulations in further comparisons. For the 3 central models, the top 10% parcels by mass in the Global statistics control 37-44% of the total reactivity for all 3 Rs; and the complementary result is that the bottom 50% parcels control only 6-10% of the total reactivity. The dominance of the high reactivity parcels is starkest for L-O3 and L-CH4 where 15% of the parcels (Atlantic or Pacific) control half of the budget, while P-O3 is distributed more evenly across the parcels, especially in the Atlantic.

These statistics are readily seen in the convex curves of sorted reactivity values in Figure 1. The mean values (open circles plotted at the 50th percentile) lie well above the median, except for Atlantic P-O3. The rapid, almost hyperbolic increases starting above the 90th percentile indicates the importance of the rare, but most reactive, parcels to the total budgets. The exception to this pattern is Atlantic L-O3, which looks more like two straight lines, breaking at the 50th percentile. In Figure 1 the agreement across all models (except GISS) is clear, indicating that the conclusion in Prather et al., 2018 (i.e., that most global chemistry models agree on the O_3 and CH_4 budgets if given the chemical composition) also holds for the ATom measured chemical composition. For P-O3, the F0AM model (red) has a lower median than the cluster of four 3D models, but the curve steepens faster at the highest Rs. These differences are probably caused by the F0AM protocol for NOx (maintain fixed NOx levels over 24 hours) versus the ATom-run protocol for the 3D models (let NOx photochemically evolve over 24 hours, see Fig. 2 of Prather et al., 2017), but they do not greatly affect the conclusions here. The shift to observed NOx with MDS_R2 – compare UCI (brown, R0) with UCI2 (black dashed, R2) – had noticeable changes only in the Pacific where P-O3 increased by 20% from the 10th to 80th percentile, but surprisingly, the Atlantic P-O3 is reduced. It is clear that the reactive chemistry of the Atlantic is distinct from that of the Pacific in ATom-1, but we could not simply identify the cause here. We conclude that accurate modeling of chemical composition of 80th and greater percentile is important, but that modest errors in the lowest 50th percentile are not consequential, effectively, some parcels matter more, as in Prather et al. (2017).

https://doi.org/10.5194/acp-2021-405
Preprint. Discussion started: 19 May 2021


Atmospheric Chemistry and Physics Discussions

How well does this ATom analysis work as a model intercomparison project? Overall, we find that most models give similar results when presented with the ATom-1 MDS. The agreement across a range of model formulations using differing levels of chemical complexity show this approach is robust. The different protocol for calculating reactivities between the 3D and box models, as well as the uncertainty in cloud fields, appear to have small impact on the overall results, but are informative regarding the minimum structural uncertainty in calculating the subsequent 24-hour reactivity of a well-measured air parcel.

3.1 Spatial heterogeneity of tropospheric reactivity.

A critical unknown for tropospheric chemistry modeling is what resolution is needed to correctly integrate the reaction rates controlling the budgets of key gases? A similar question was addressed in Yu et al. (2016) for the isoprene oxidation pathways using a model with variable resolution (500 km, 250 km, and 30 km) compared to aircraft measurements. ATom's 10 s air parcels measure 2 km (horizontal) by 80 m (vertical) during most profiles. These 10 s parcels have similar variability to that seen on the 1 s scale (200 m by 8 m, see Figure S2). An interesting parallel result from the RDS statistics is that there are not enough extremely rare parcels with high enough reactivity to distort the average. While the sorted reactivity curves (Figure 1, Tables 2 & S8) continue to steepen from the 90^{th} to 97^{th} percentile, the slope does not change that much: the top 3% parcels contribute to about 8-15% of the total reactivity over the Pacific and Atlantic Basins. Thus, if our modeling misses the top 1% of reactive air parcels, for example due to the inability to simulate intensely reactive thin pollution layers, then we miss at most 5% of the total reactivity. This finding is new and encouraging, and it needs to be verified with the ATom-2, 3, and 4 data. The other question is whether the 3D models with 100 km by 500 m cells can even match the statistical distributions measured at 2 km by 80 m. There is some encouraging information from the sample descent profile shown in Figure S2: the reactivities for this profile change slowly over the 500-m intervals marked on the plot, and thus the models may capture much of the variance.

The curtain plots of Figure 2 follow the profiling of ATom-1 in the Central Pacific, Eastern Pacific, and Atlantic tropical domains. The UCI RDS_R2 are averaged and plotted in 1° latitude by 200 m thick cells, and thus some of the small scale heterogeneity is lost here. We separate the Eastern (121°W, research flight (RF) 1) from the Central Pacific (RF 3, 4 and 5) because we are looking for contiguous latitude-by-pressure structures. In the Central Pacific (row 1), highly reactive (hot) P-O3 parcels (> 6 ppb/day) occur in a partially resolved air mass at latitudes 20-22°N and pressure altitudes 2-3 km, and in more scattered parcels (> 3 ppb/day) below 5 km down to 20°S. High L-O3 and L-CH4 coincide with this 20-22°N air mass, and also with some high P-O3 at lower latitudes. This pattern of overlapping extremes in all 3 Rs is surprising because the models' mid-Pacific climatologies show a separation between regions of high L-O3 and high P-O3 (Figure 3 of Prather et al., 2017). In contrast to the pattern here, the modeled P-O3 tends to peak in the upper troposphere and the marine boundary layer, reflecting perhaps the models' parameterizations used to distribute lightning NOx. The ATom profiling seems to catch similarly reactive parcels in adjacent profiles separate by a few hundred km, scales easily resolvable with 3D models.

In the Eastern Pacific (row 2), the overlap of outbound and return profiles enhances the spatial sampling over the 10 h flight. The region of very large L-O3 (> 5 ppb/day) is extensive, beginning at 5-6 km at 10°N and broadening to 2-8 km at 28°N. The region of L-CH4 is similar, but loss at higher altitudes is attenuated, because of the temperature dependence of L-CH4 and possibly because of differing OH:HO_2 ratios with altitude. Large P-O3 (> 6 ppb/day) occurs in

https://doi.org/10.5194/acp-2021-405
Preprint. Discussion started: 19 May 2021


Atmospheric Chemistry and Physics Discussions

some but not all of these highly reactive regions, suggesting that NOx is not as evenly distributed as is HOx. P-O3 also show regions of high reactivity above 8 km that are not in the high L-O3 and L-CH4 regions, probably evidence of convective sources of HOx and NOx, but too cold and dry for the L-O3 and L-CH4 reactions. ATom-1 RF1 (29 Jul 2016) occurred during the North American Monsoon when there was easterly flow off Mexico, thus the high reactivity of this large air mass indicates that continental deep convection is a source of high reactivity for both O_3 and CH_4.

In the Atlantic (row 3) we see similar air masses through successive profiles again, particularly in the northern tropics. The Atlantic P-O3 shows high-altitude reactivity similar to the Eastern Pacific. Likewise, the large values of L-O3 and L-CH4 match the Eastern Pacific and not Central Pacific. Unlike either Pacific transect, the Atlantic L-O3 and L-CH4 show some high reactivity below 1 km altitude. Overall, the ATom-1 profiling clearly identifies extended air masses of high L-O3 and L-CH4 extending over 2-5 km in altitude and 10° of latitude. The high P-O3 regions tend to be much more heterogeneous with greatly reduced spatial extent.

Overall, the extensive ATom profiling identifies a highly heterogeneous mix of chemical composition in the tropical Atlantic and Pacific with a large range of reactivities. What is important for those trying to model tropospheric chemistry is that the spatial scales of variability are within the capability of modern global models.

3.2 Testing model climatologies.

The ATom data set, including its derived RDS, provide a unique opportunity to test models, both chemistry-transport (CTM) and chemistry-climate models (CCMs). As a first look, we make this comparison using ATom-1 data and the modeled chemical statistics for mid-August used in Prather et al. (2017). The complex patterns of the 3Rs seen in Figure 2 cannot be matched directly with CCMs and thus we seek simpler statistics combining average profiles with probability distributions. The mean profiles of the 3Rs from the Figure 2 tropical ocean are compared with the 6 models in Figure 3.

For P-O3 (top row), the discrepancy between models and measurements is stark. In the Central Pacific at 8-12 km, the ATom-1 results tend to agree with models, showing ozone production of about 1 ppb/day. Below 8 km, ATom's P-O3 increases to a peak of 4 ppb/day at 2 km, while the models' P-O3 stay constant down to 4 km and then decrease to about 0.5 ppb/day below 2 km. This pattern indicates that in the middle of the Pacific, the NOx+HOx combination that produces ozone is suppressed throughout the lower troposphere in the models. In the Eastern Pacific and Atlantic, both models' and ATom reactivities indicate that that P-O3 is greatly enhanced above 6 km as compared to the Central Pacific, but below 6 km the ATom P-O3 are much larger than that of the models', by a factor of 2. In the upper troposphere, the agreement indicates that both models and ATom find the influence of deep continental convection bringing reactive NOx+HOx air masses to the nearby oceanic regions, but not to the mid Pacific. The difference below 5 km in all 3 regions implies a consistent bias across the models in some combination of HOx sources and/or the vertical redistribution of lightning NOx. This difference is unlikely to be a sampling bias in ATom, given it occurs in all 3 regions.

For L-O3 (middle row), the agreement in the Central Pacific is very good throughout the 0-12 km range. Moving to the Eastern Pacific and Atlantic, both models and ATom show increased reactivity consistent with continental convective outflow. The excess ATom reactivity in the Eastern Pacific (3-8 km) is clear in Figure 2 and likely due to easterly mid-tropospheric flow from

https://doi.org/10.5194/acp-2021-405
Preprint. Discussion started: 19 May 2021


Atmospheric Chemistry and Physics Discussions

315 convection over Mexico at that specific time (29 July 2016). Similarly, the ATom excess
316 reactivity at low-level (1-3 km) in the Atlantic is associated with biomass burning in Africa and
317 was measured in other trace species. Thus, in terms of L-O3, the ATom-model differences may
318 be due to specific meteorological conditions and this could be tested with CTMs using 2016
319 meteorology and wildfires.

320 For L-CH4 (bottom row), the ATom-model pattern is similar to L-O3, but the excess ATom
321 reactivity occurs at lower altitudes. Overall, the ATom L-CH4 is slightly greater than the
322 modeled L-CH4. L-O3 is dominated by O(1D) and HO_2 loss, while L-CH4 is limited to OH loss.
323 Increases in NOx shift the HOx balance to OH, and we see that in the 1-2 km region of peak P-
324 O3 in the Pacific, but less so in the Atlantic. Overall, there is clear evidence that the Atlantic and
325 Pacific have very different chemical mixtures controlling the reactivities and that convection over
326 land (monsoon or biomass burning) creates air masses that are still highly reactive a day or so
327 later.

328 Mean profiles do not reflect the heterogeneity seen in Figure 2, and so we also examine the
329 statistical distribution of reactivities underlying the profiles in Figure 3, as shown in supplemental
330 Figure S7. The frequency of occurrence uses the same weighting as before with 0.5 ppb/d bins
331 (0.25 ppb/d for L-CH4). The model climatologies (6 colors) show a monotonically decreasing
332 frequency that mostly matches the ATom statistics. The obvious discrepancy is with P-O3 in
333 both Pacific and Atlantic basins. ATom data has very low occurrence of P-O3 < 1 ppb/d and a
334 broad, almost uniform frequency (~0.1) extending out to 4 ppb/d. This result is consistent with
335 the mean profile errors (Figure 3) and emphasizes where the error is occurring. The match for L-
336 CH4 is excellent in both basins, although the models have a greater occurrence in the 0.5-1.5
337 ppb/d middle range, and reduced occurrence in the higher 1.5-2.5 ppb/d range. For L-O3, the
338 match is very good and similar, with models overestimating the middle range (1-3 ppb/d) and
339 missing the upper range (>5 ppb/d). The frequency of reactivities greater than the plot range is
340 included in the last point, and for L-O3 the ATom parcels have a large occurrence of L-O3 > 6
341 ppb/d that is not seen in the models (except GISS). Similar results apply to P-O3. For the
342 Pacific, both Central and Eastern have been combined (black line), but a separate line (grey)
343 including only the Central Pacific is also shown. It is clear that the extreme reactivities are in the
344 Eastern Pacific, as is evident from Figure 2.

345 The ability to test the model's reactivity statistics with the ATom 10 s data is not obvious. The
346 disconnect between statistics for 2-km parcels versus 100-km grid cells is likely. If there is
347 significant chemical variability at scales below 50 km, then the averaging occurring in model grid
348 cells would greatly alter the frequencies. For example, in Figure S8, we take the Pacific P-O3
349 frequency (black), generate a random set of points from that distribution, and then start averaging
350 adjacent points in groups (2, 4, 8; denoted as 4 km, 8km, 16 km). The resulting statistics rapidly
351 evolve into a Gaussian-like distribution about the mean value. Thus, the ability to nearly match
352 the ATom-1 statistics with our global chemistry models is significant, and we cannot explain the
353 P-O3 discrepancy as a model-averaging problem.

354 This deficit in modeled P-O3 points to a NOx deficiency in the models, and this is clear in the
355 comparison of the probability distribution histograms for NOx shown in Figure 4. In the Central
356 Pacific over 0-12 km (1st row), ATom has a reduced frequency of parcels with 2-20 ppt and
357 corresponding increase in parcels with 20-80 ppt. This discrepancy is amplified in the lower
358 troposphere, 0-4 km (2nd row). In the middle of the Pacific our chemistry models are missing a
359 large, local source of NOx. The obvious source is lightning since oceanic sources of organo-
360 nitrates as measured on ATom could not supply this amount. The distribution of NOx throughout

https://doi.org/10.5194/acp-2021-405
Preprint. Discussion started: 19 May 2021


Atmospheric Chemistry and Physics Discussions

the troposphere also indicates a lightning-related source that is vertically mixed. In the Eastern Pacific, the ATom 0-4 km troposphere appears again to have large amounts of air with 20-50 ppt, while the full troposphere more closely matches the models except for the large occurrence of air with 100-300 ppt NOx. These high-NOx regions are probably direct outflow from very deep convection with lightning in the monsoon regions over Mexico at this time. In the Atlantic, the modeled NOx shows too frequent occurrence of low NOx (<10 ppt) and thus underestimates the 10-100 ppt levels at all altitudes. ATom has a strong peak occurrence about 80-120 ppt in the upper troposphere and, like the East Pacific, this is probably due to lightning NOx from deep convection over land (Africa or South America). The models appear to be missing significant NOx sources throughout the tropics, especially below 4 km.

In Figure 4 we also look at the histograms for the key HOx-related species HOOH (3rd row) and HCHO (4th row). For these species, the ATom-model agreement is generally good. If anything, the models tend to have too much HOOH: ATom shows systematically large occurrences of low HOOH (50-200 ppt, especially Central Pacific) indicating, perhaps, that convective or cloud scavenging of HOOH is more effective than is modeled. HCHO shows reasonable agreement in the Atlantic, but in both Central and Eastern Pacific, the modeled low-end (<40 ppt) is simply not seen in the ATom data. Also, the models are missing a strong HCHO peak at 300 ppt in the Eastern Pacific. Thus, in terms of these HOx precursors, the model climatologies appear to be at least as reactive as the ATom data.

While the ATom-1 data in Figure 4 is limited to a single transect, the model discrepancies apply across the three tropical regions, and the simple chemical statistics for these flights are probably enough to identify measurement-model discrepancies in a climatological sense and focusing on specific abundance ranges. For the individual models, a more thorough comparison with these and other key species (e.g., CO, O_3, H_2O, CH_3OOH, PAN, C_2H_6) is likely to identify areas for model development. An encouraging result here is that where individual models tend to deviate from their peers, they also deviate from the ATom-1 probability distributions. In most cases (but not NOx), the models match the first-order statistics from ATom.

Some of the structure in these chemical distributions is driven by large-scale physics, such as the cold and dry upper troposphere having low HOOH and HCHO levels and reactivities < 1 ppb/d. Nevertheless, however one parses these statistical comparisons in Figures 4 and S7, it appears that current global chemistry models with resolutions of about 100 km by 500 m can resolve much of the wide range of chemical heterogeneity in the atmosphere, which for the oceanic transects is, we believe, adequately resolved by the 10 s ATom measurements.

4.Conclusion

This paper opens the door for what can be done by the community with the publicly available ATom data. The mix of key species that allows us to calculate the reactivity of the air parcels is near unique. We find that the reactivity of the troposphere with respect to O_3 and CH_4 is dominated by a fraction of the air parcels, but not by so small and infrequent a fraction as to challenge the resolution of current CTMs to simulate these observations. In comparing ATom results with modeled climatologies, we find a clear model error, missing O_3 production over the tropical oceans' lower troposphere, and traced it to the lack of NOx below 4 km. The occurrence of the same error over the Central and Eastern Pacific as well as the Atlantic Ocean makes this a robust model-measurement discrepancy.

https://doi.org/10.5194/acp-2021-405
Preprint. Discussion started: 19 May 2021


Atmospheric Chemistry and Physics Discussions

Building our chemical statistics from the ATom 10 s air parcels on a scale of 2 km by 80 m, we can identify the fundamental scales of spatial heterogeneity in tropospheric chemistry. Although heterogeneity occurs at the finest scales (such as seen in some 1 s observations) the majority of variability in terms of the O_3 and CH_4 budgets occurs across scales larger than neighboring 2 km parcels. It appears to be largely resolved by the models' 100 km by 500 m grid cells. This surprising result is evident by the similarity of many of the ATom 1D probability densities – both species and reactivities – with those from the models' August climatologies. These comparisons show that the modeled chemical heterogeneity is consistent with the innate heterogeneity of the troposphere as measured by the 10 s parcels in ATom. A similar conclusion for biomass burning smoke particles is found by Schill et al (2020), where the most of the smoke appears in the background rather than in pollution plumes, and therefore much of the variability occurs on synoptic scales resolved by global models (see their Figure 1 compared with Figure 2 here).

As a quick look at the opportunities provided by the ATom data, we present an example based on Wolfe et al (2019), who used the F0AM model and semi-analytical arguments to show that troposphere HCHO columns (measurable by satellite and ATom) are related to OH columns (measured by ATom) and thus to CH_4 loss. Figure 5 extends the Wolfe et al study using the individual air parcels and plotting L-CH4 (ppb/d) versus HCHO (ppt) for the 3 tropical regions where most of the CH_4 loss occurs. The relationship is linear with slopes ranging from 4 to 6 /d, but the largest reactivities (0-4 km, 1-3 ppb/d) are not so well correlated with HCHO.

Decadal scale shifts in the budgets of O_3 and CH_4 are likely to be evident through the statistical patterns of the key species, rather than simply via average profiles. The underlying design of ATom was to collect enough data to develop such a multivariate chemical climatology. As a quick look, we show the joint probability distribution on a logarithmic scale as in Prather et al. (2017) for HOOH and NOx in Supplemental Figure S6. The patterns for the tropical Central Pacific are quite similar for the 4 seasons of ATom deployments and the fitted ellipses are almost identical for ATom 2, 3, and 4. Thus, for these species in the Central Pacific, we believe that ATom provides a benchmark of the 2016-2018 chemical state, one that can be revisited with an aircraft mission in a decade to detect changes in not only chemical composition but also reactivity.

ATom identifies which 'highly reactive' spatial or chemical environments could be targeted in future campaigns for process studies or to provide a better link between satellite observations and photochemical reactivity. The many corollary species measured by ATom (not directly involved in CH_4 and O_3 chemistry) provide clues to the origin or chemical processing of these environments.

As is usual with a new model intercomparison projects, we find new model features and identify errors. In the UCI model a lumped alkane formulation (averaging alkanes C_3H_8 and higher) did not show up in Prather et al. (2018) where UCI supplied all the species, but when the ATom data were used, the UCI model became an outlier. Once found, this problem was easily fixed. The anomalous GISS results have been examined by a co-author, but no clear causes have been identified as of this publication. Inclusion of the F0AM model here for the reactivity calculations provided an interesting contrast with the A-run simulations of the global CCM/CTMs as described in Prather et al. (2017). We hope to engage a wider modeling community beyond the ATom science team, as in Hall et al. (2018), in the calculation of photochemical processes and budgets based on the ATom measurements.

https://doi.org/10.5194/acp-2021-405
Preprint. Discussion started: 19 May 2021

Atmospheric Chemistry and Physics Discussions

Data Availability. The MDS and RDS data for ATom 1, 2, 3, and 4 are presented here as core ATom deliverables, and are now posted on the NASA ESPO ATom website (https://espo.nasa.gov/atom/content/ATom) and will be archived at the ORNL DAAC alongside the 10 s ATom merged measurements. Details of the ATom mission and data sets are found on the NASA mission web site (https://espo.nasa.gov/atom/content/ATom) and at the final archive at Oak Ridge National Laboratory (ORNL; https://daac.ornl.gov/ATOM/guides/ATom_merge.html). The Matlab codes and data sets used in the analysis here are posted on Dryad (https://doi.org/10.7280/D1Q699).

Author Contributions:

H.G., C.M.F, S.C.W., and M.J.P. designed the research and performed the data analysis; S. A. S., S. D. S., L. E., F. L., J. L., A. M. F., G. C., L. T. M., and G. W., contributed original atmospheric chemistry model results; G. W., M. K., J. C., G. D., J. D., B. C. D., R. C., K. M., J. P., T. B. R., C. T., T. F. H., D. B., N. J. B., E. C. A., R. S. H., J. E., E. H., and F. M. contributed original atmospheric observations; H.G., C.M.F, and M.J.P. wrote the paper.

Competing Interest Statement: No.

Acknowledgments

The authors are indebted to the entire ATom Science Team including the managers, pilots and crew who made this mission possible. Many other scientists not on the author list enabled the measurements and model results used here. Primary funding of the preparation of this manuscript at UC Irvine was through NASA grant NNX15AG57A.

https://doi.org/10.5194/acp-2021-405
Preprint. Discussion started: 19 May 2021

Atmospheric Chemistry and Physics Discussions

References

Burkholder, J. B., Sander, S. P., Abbatt, J. P. D., Barker, J. R., Huie, R. E., Kolb, C. E., Kurylo, M. J., Orkin, V. L., Wilmouth, D. M. and Wine, P. H., 2015. Chemical kinetics and photochemical data for use in atmospheric studies: evaluation number 18. Pasadena, CA: Jet Propulsion Laboratory, National Aeronautics and Space Administration (2015).

Douglass, A.R., Prather, M.J., Hall, T.M., Strahan, S.E., Rasch, P.J., Sparling, L.C., Coy, L. and Rodriguez, J.M., 1999. Choosing meteorological input for the global modeling initiative assessment of high‐speed aircraft. Journal of Geophysical Research: Atmospheres, 104(D22), pp.27545-27564.

Eastham, S.D. and Jacob, D.J., 2017. Limits on the ability of global Eulerian models to resolve intercontinental transport of chemical plumes. Atmospheric Chemistry and Physics, 17(4), pp.2543-2553.

Griffiths, P.T., Murray, L.T., Zeng, G., Shin, Y.M., Abraham, N.L., Archibald, A.T., Deushi, M., Emmons, L.K., Galbally, I.E., Hassler, B. and Horowitz, L.W., 2021. Tropospheric ozone in CMIP6 Simulations. Atmospheric Chemistry and Physics, 21(5), pp.4187-4218.

Hall, S.R., Ullmann, K., Prather, M.J., Flynn, C.M., Murray, L.T., Fiore, A.M., Correa, G., Strode, S.A., Steenrod, S.D., Lamarque, J.F. and Guth, J., 2018. Cloud impacts on photochemistry: building a climatology of photolysis rates from the Atmospheric Tomography mission. Atmospheric Chemistry and Physics, 18(22), pp.16809-16828.

Heald, C.L., Coe, H., Jimenez, J.L., Weber, R.J., Bahreini, R., Middlebrook, A.M., Russell, L.M., Jolleys, M., Fu, T.M., Allan, J.D. and Bower, K.N., 2011. Exploring the vertical profile of atmospheric organic aerosol: comparing 17 aircraft field campaigns with a global model. Atmospheric Chemistry and Physics, 11(24), pp.12673-12696.

Myhre, G., Shindell, D. and Pongratz, J., 2014. Anthropogenic and Natural Radiative Forcing, in Climate Change 2013: The Physical Science Basis, IPCC WGI Contribution to the Fifth Assessment Report, edited by T. F. Stocker, D. Qin and et al. (Cambridge University Press), pp. 659-740.

Naik, V., Voulgarakis, A., Fiore, A.M., Horowitz, L.W., Lamarque, J.F., Lin, M., Prather, M.J., Young, P.J., Bergmann, D., Cameron-Smith, P.J. and Cionni, I., 2013. Preindustrial to present-day changes in tropospheric hydroxyl radical and methane lifetime from the Atmospheric Chemistry and Climate Model Intercomparison Project (ACCMIP). Atmospheric Chemistry and Physics, 13(10), pp.5277-5298.

Prather, M.J., Ehhalt, D., Dentener, F., Derwent, R., Dlugokencky, E.J., Holland, E., Isaksen, I., Katima, J., Kirchhoff, V., Matson, P. and Midgley, P., 2001. Chapter 4 - Atmospheric Chemistry and Greenhouse Gases, Climate Change 2001: The Scientific Basis. Third Assessment Report of the Intergovernmental Panel on Climate Change., 239-287.

Prather, M.J., Zhu, X., Flynn, C.M., Strode, S.A., Rodriguez, J.M., Steenrod, S.D., Liu, J., Lamarque, J.F., Fiore, A.M., Horowitz, L.W. and Mao, J., 2017. Global atmospheric chemistry–which air matters. Atmospheric Chemistry and Physics, 17(14), pp.9081-9102.

https://doi.org/10.5194/acp-2021-405
Preprint. Discussion started: 19 May 2021

Atmospheric Chemistry and Physics Discussions

Prather, M.J., Flynn, C.M., Zhu, X., Steenrod, S.D., Strode, S.A., Fiore, A.M., Correa, G., Murray, L.T. and Lamarque, J.F., 2018. How well can global chemistry models calculate the reactivity of short-lived greenhouse gases in the remote troposphere, knowing the chemical composition. Atmospheric Measurement Techniques, 11(5), pp.2653-2668.

Rastigejev, Y., Park, R., Brenner, M.P. and Jacob, D.J., 2010. Resolving intercontinental pollution plumes in global models of atmospheric transport. Journal of Geophysical Research: Atmospheres, 115(D2).

Schill, G.P., Froyd, K.D., Bian, H., Kupc, A., Williamson, C., Brock, C.A., Ray, E., Hornbrook, R.S., Hills, A.J., Apel, E.C. and Chin, M., 2020. Widespread biomass burning smoke throughout the remote troposphere. Nature Geoscience, 13(6), pp.422-427.

Stevenson, D.S., Dentener, F.J., Schultz, M.G., Ellingsen, K., Van Noije, T.P.C., Wild, O., Zeng, G., Amann, M., Atherton, C.S., Bell, N. and Bergmann, D.J., 2006. Multimodel ensemble simulations of present‐day and near‐future tropospheric ozone. Journal of Geophysical Research: Atmospheres, 111(D8).

Stevenson, D.S., Young, P.J., Naik, V., Lamarque, J.F., Shindell, D.T., Voulgarakis, A., Skeie, R.B., Dalsoren, S.B., Myhre, G., Berntsen, T.K. and Folberth, G.A., 2013. Tropospheric ozone changes, radiative forcing and attribution to emissions in the Atmospheric Chemistry and Climate Model Intercomparison Project (ACCMIP). Atmospheric Chemistry and Physics, 13(6), pp.3063-3085.

Stevenson, D.S., Zhao, A., Naik, V., O'Connor, F.M., Tilmes, S., Zeng, G., Murray, L.T., Collins, W.J., Griffiths, P.T., Shim, S. and Horowitz, L.W., 2020. Trends in global tropospheric hydroxyl radical and methane lifetime since 1850 from AerChemMIP. Atmospheric Chemistry and Physics, 20(21), pp.12905-12920.

Stocker, T.F., Qin, D., Plattner, G.K., Tignor, M., Allen, S.K., Boschung, J., Nauels, A., Xia, Y., Bex, V. and Midgley, P.M., 2013. Contribution of working group I to the fifth assessment report of the intergovernmental panel on climate change. Climate change(Cambridge University Press., 2013), pp.33-115.

Tie, X., Brasseur, G. and Ying, Z., 2010. Impact of model resolution on chemical ozone formation in Mexico City: application of the WRF-Chem model. Atmospheric Chemistry and Physics, 10(18), pp.8983-8995.

Voulgarakis, A., Naik, V., Lamarque, J.F., Shindell, D.T., Young, P.J., Prather, M.J., Wild, O., Field, R.D., Bergmann, D., Cameron-Smith, P. and Cionni, I., 2013. Analysis of present day and future OH and methane lifetime in the ACCMIP simulations. Atmospheric Chemistry and Physics, 13(5), pp.2563-2587.

Wofsy, S.C., Afshar, S., Allen, H.M., Apel, E.C., Asher, E.C., Barletta, B., Bent, J., Bian, H., Biggs, B.C., Blake, D.R. and Blake, N., 2018. ATom: Merged atmospheric chemistry, trace gases, and aerosols. ORNL DAAC Oak Ridge, Tennessee, USA. https://doi.org/10.3334/ORNLDAAC/1581,.

Wofsy, S.C., 2011. HIAPER Pole-to-Pole Observations (HIPPO): fine-grained, global-scale measurements of climatically important atmospheric gases and aerosols. Philosophical

https://doi.org/10.5194/acp-2021-405
Preprint. Discussion started: 19 May 2021

Atmospheric Chemistry and Physics Discussions

552 Transactions of the Royal Society A: Mathematical, Physical and Engineering Sciences,
553 369(1943), pp.2073-2086.

554 Wolfe, G.M., Nicely, J.M., Clair, J.M.S., Hanisco, T.F., Liao, J., Oman, L.D., Brune, W.B.,
555 Miller, D., Thames, A., Abad, G.G. and Ryerson, T.B., 2019. Mapping hydroxyl variability
556 throughout the global remote troposphere via synthesis of airborne and satellite formaldehyde
557 observations. Proceedings of the National Academy of Sciences, 116(23), pp.11171-11180.

558 Young, P.J., Archibald, A.T., Bowman, K.W., Lamarque, J.F., Naik, V., Stevenson, D.S., Tilmes,
559 S., Voulgarakis, A., Wild, O., Bergmann, D. and Cameron-Smith, P., 2013. Pre-industrial to end
560 21st century projections of tropospheric ozone from the Atmospheric Chemistry and Climate
561 Model Intercomparison Project (ACCMIP). Atmospheric Chemistry and Physics, 13(4), pp.2063-
562 2090.

563 Young, P.J., Naik, V., Fiore, A.M., Gaudel, A., Guo, J., Lin, M.Y., Neu, J.L., Parrish, D.D.,
564 Rieder, H.E., Schnell, J.L. and Tilmes, S., 2018. Tropospheric Ozone Assessment Report:
565 Assessment of global-scale model performance for global and regional ozone distributions,
566 variability, and trends. Elementa: Science of the Anthropocene, 6.

567 Yu, K., Jacob, D.J., Fisher, J.A., Kim, P.S., Marais, E.A., Miller, C.C., Travis, K.R., Zhu, L.,
568 Yantosca, R.M., Sulprizio, M.P. and Cohen, R.C., 2016. Sensitivity to grid resolution in the
569 ability of a chemical transport model to simulate observed oxidant chemistry under high-isoprene
570 conditions. Atmospheric Chemistry and Physics, 16(7), pp.4369-4378.

571 Zhuang, J., Jacob, D.J. and Eastham, S.D., 2018. The importance of vertical resolution in the free
572 troposphere for modeling intercontinental plumes. Atmospheric Chemistry and Physics, 18(8),
573 pp.6039-6055.

574

https://doi.org/10.5194/acp-2021-405
Preprint. Discussion started: 19 May 2021

Atmospheric Chemistry and Physics Discussions

Figures and Tables

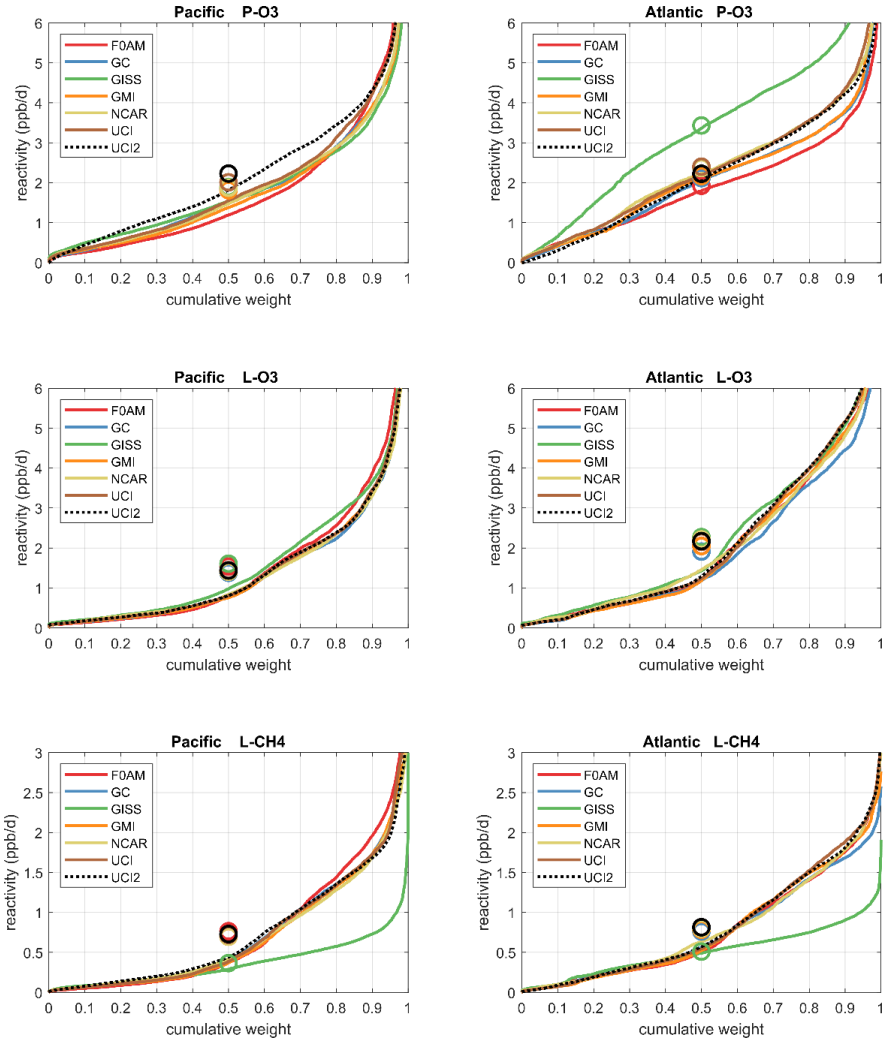

Figure 1. Sorted reactivities (P-O3, L-O3, L-CH4, ppb/day) for the Pacific and Atlantic domains of ATom-1. Each parcel is weighted, see text. The six modeled reactivities for MDS_R0 are shown with colored lines and the UCI calculation for MDS_R2 is shown as a black dashed line. The mean value for each model is shown with an open circle plotted at the 50th percentile. (Flip about the axes and it is a cumulative probability density function.)

https://doi.org/10.5194/acp-2021-405
Preprint. Discussion started: 19 May 2021

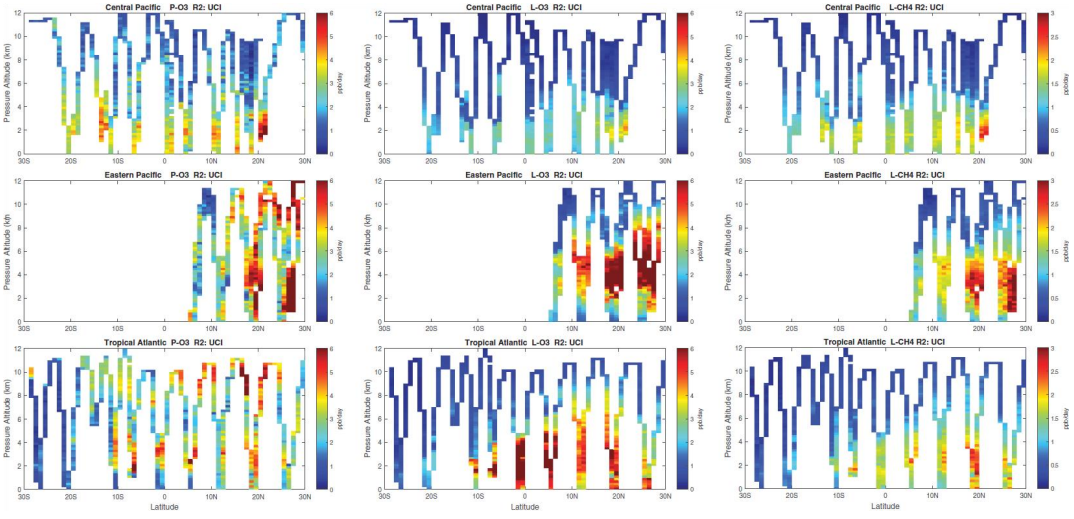

585

586 **Figure 2**. Curtain plots for P-O3 (0-6 ppb/d), L-O3 (0-6 ppb/d) and L-CH4 (0-3 ppb/d) showing
587 the profiling of ATom-1 flights in the central Pacific (RF 3, 4 and 5), eastern Pacific (RF 1), and
588 Atlantic (RF 7, 8, and 9). Reactivities are calculated for MDS_R2 with the UCI CTM. The 10 s
589 air parcels are averaged into 1° latitude and 200 m bins.

590

591

592

https://doi.org/10.5194/acp-2021-405
Preprint. Discussion started: 19 May 2021

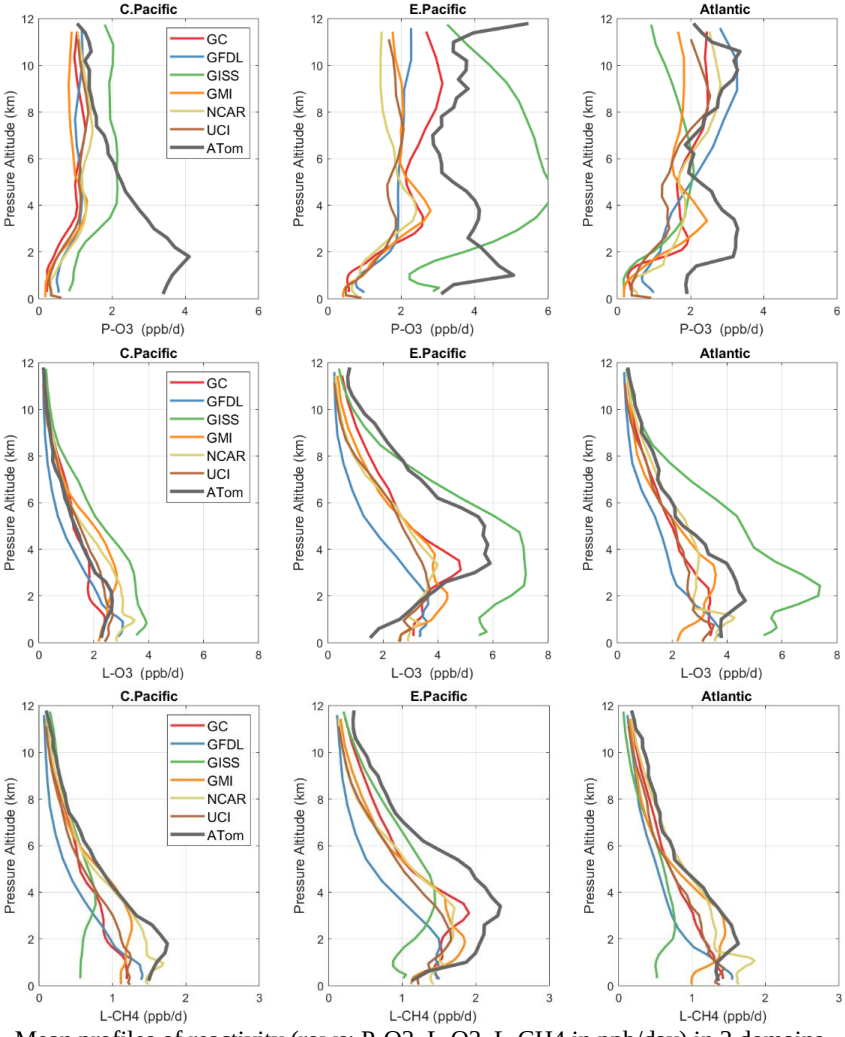

Figure 3. Mean profiles of reactivity (rows: P-O3, L-O3, L-CH4 in ppb/day) in 3 domains (columns: C. Pacific, 30°S-30°N by 180-210°E; E. Pacific, 0-30°N by 230-250°E; Atlantic, 30°S-30°N by 326-343°E). ATom-1 (gray) results are from **Figure 2**, while model results are taken from the August climatologies in Prather et al. (2017).

593

594

https://doi.org/10.5194/acp-2021-405
Preprint. Discussion started: 19 May 2021

Atmospheric Chemistry and Physics Discussions

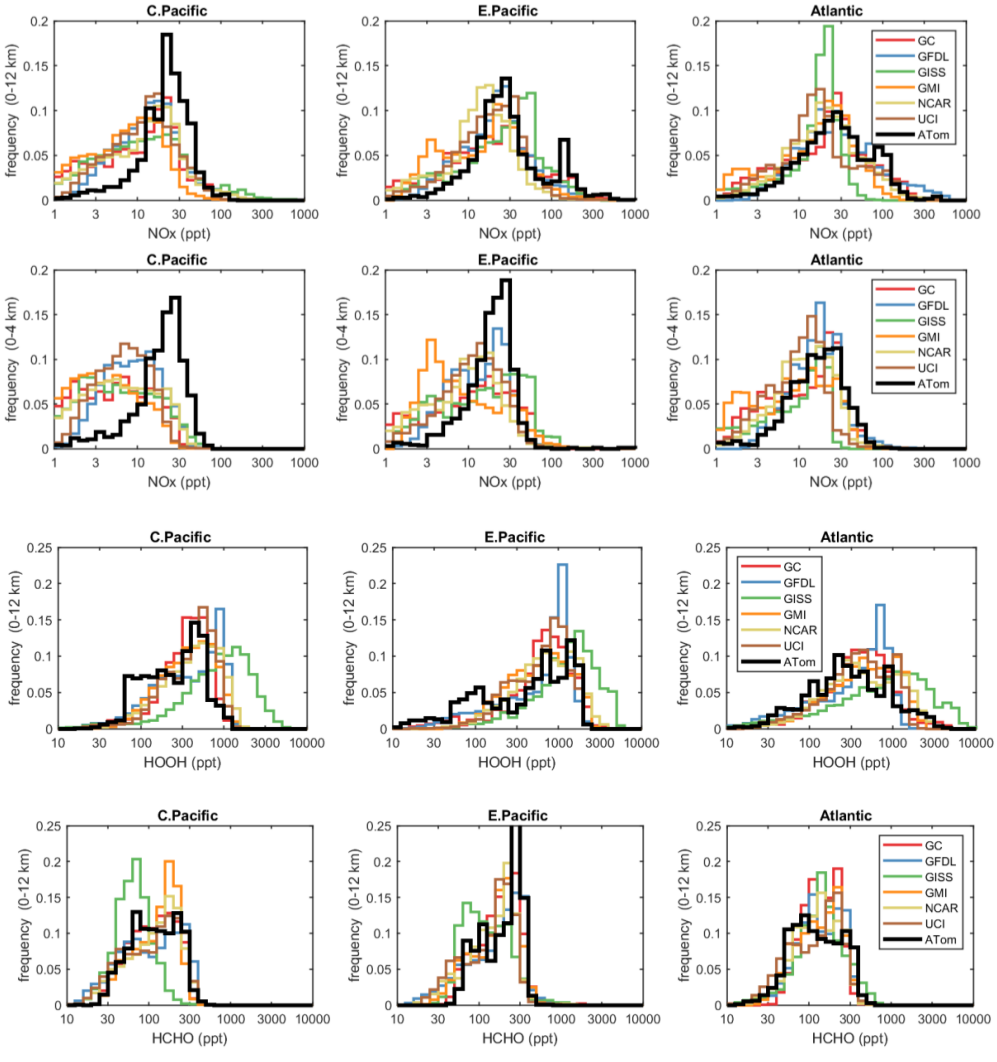

Figure 4. Histograms of probability distributions (PDs) of NO_x (0-12 km, row 1), NO_x (0-4 km, row 2), HOOH (0-12 km, row 3), and HCHO (0-12 km, row 4) for the 3 tropical regions (Central Pacific, Eastern Pacific, Atlantic). All species are binned in ppt, uniform on a log scale. The weighting of air parcels is described in the text. The ATom-1 data is plotted on top of the 6 global chemistry models' results for a day in mid-August and sampled for the regions used in **Figure 3**.

https://doi.org/10.5194/acp-2021-405
Preprint. Discussion started: 19 May 2021

Atmospheric Chemistry and Physics Discussions

605

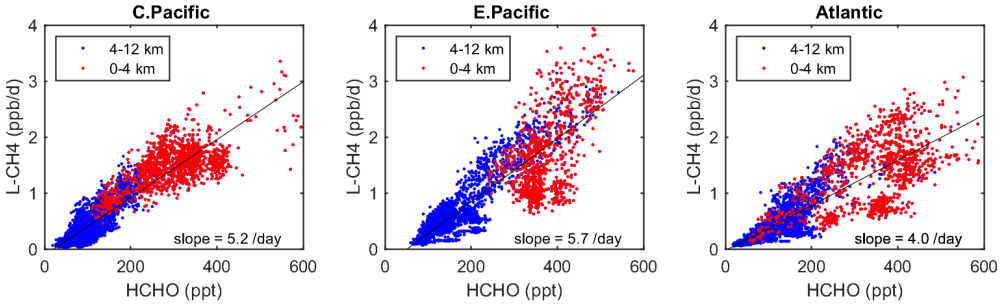

606

607

608 **Figure 5**. Scatterplot of L-CH4 (ppb/d) versus HCHO (ppt) for ATom 1 in the 3 tropical regions
609 shown in **Figure 3**. The air parcels are split into lower troposphere (0-4 km pressure altitude, red
610 dots) where most of the reactivity lies and mid+upper troposphere (4-12 km, blue). A simple
611 linear fit to all data is shown (thin black line) and the slope is given in units of 1/day.

612

613

614

https://doi.org/10.5194/acp-2021-405
Preprint. Discussion started: 19 May 2021

Atmospheric Chemistry and Physics Discussions

Table 1. Chemistry models

Used in	ID	Model name	Model type	Meteorology	Model Grid
clim, R0	GFDL	GFDL-AM3	CCM	NCEP (nudged)	C180 x L48
clim, R0	GISS	GISS-E2.1	CCM	Daily SSTs, nudged to MERRA	2° x 2.5° x 40L
clim, R0, R1	GMI	GMI-CTM	CTM	MERRA	1° x 1.25° x 72L
clim, R0	GC	GEOS-Chem	CTM	MERRA-2	2° x 2.5° x 72L
clim, R0	NCAR	CAM4-Chem	CCM	MERRA	0.47° x 0.625° x 52L
clim, R0, R1, R2	UCI	UCI-CTM	CTM	ECMWF IFS Cy38r1	T159N80 x L60
R0	F0AM	F0AM	box	MDS+scaled ATom Js	N/A

615

616

https://doi.org/10.5194/acp-2021-405
Preprint. Discussion started: 19 May 2021

Atmospheric Chemistry and Physics Discussions

617

Table 2. Reactivity statistics for the 3 large domains (Global, Pacific, Atlantic).

Value	Region	Models with R0								Models with R2	
		F0AM	GC	GISS	GMI	NCAR	UCI	U15	U97	GMI1	UCI2
P-O3, mean, ppb/d											
	Global	1.83	1.58	1.98	1.53	1.64	1.75	1.75	1.75	1.75	1.83
	Pacific	1.96	1.97	2.00	1.92	1.99	2.13	2.09	2.10	2.19	2.35
	Atlantic	2.11	2.29	3.73	2.38	2.57	2.61	2.60	2.61	2.74	2.63
L-O3, mean, ppb/d											
	Global	1.55	1.17	1.39	1.22	1.24	1.27	1.27	1.27	1.23	1.29
	Pacific	1.62	1.46	1.69	1.49	1.52	1.53	1.49	1.51	1.48	1.53
	Atlantic	2.32	2.17	2.57	2.36	2.43	2.48	2.47	2.49	2.39	2.51
L-CH4, mean, ppb/d											
	Global	0.68	0.53	0.32	0.52	0.51	0.55	0.55	0.55	0.55	0.56
	Pacific	0.81	0.76	0.39	0.74	0.75	0.77	0.75	0.76	0.77	0.78
	Atlantic	0.90	0.88	0.57	0.92	0.90	0.95	0.95	0.95	0.96	0.97
P-O3, %of total R in top 10%											
	Global	38%	38%	36%	38%	37%	40%	40%	40%	38%	37%
	Pacific	35%	28%	27%	29%	28%	30%	29%	29%	28%	26%
	Atlantic	22%	22%	20%	22%	21%	23%	23%	23%	21%	21%
L-O3, %of total R in top 10%											
	Global	39%	44%	41%	44%	43%	45%	45%	45%	45%	44%
	Pacific	36%	34%	32%	35%	33%	34%	34%	34%	36%	34%
	Atlantic	26%	25%	25%	25%	28%	26%	26%	26%	25%	26%
L-CH4, %of total R in top 10%											
	Global	37%	39%	33%	40%	39%	41%	41%	41%	41%	39%
	Pacific	35%	30%	26%	32%	30%	31%	31%	31%	31%	29%
	Atlantic	25%	23%	19%	23%	24%	24%	24%	24%	24%	24%

Global includes all ATom-1 parcels (32,383), Pacific considers all measurements (11,486) over the Pacific Ocean from 54°S to 60°N, and Atlantic uses parcels from 54°S to 60°N over the Atlantic basin (7,501). All parcels are weighted at described in the text, including a cosine(latitude) factor. See expanded Table S1.

618

https://doi.org/10.5194/acp-2021-405
Preprint. Discussion started: 19 May 2021

Atmospheric Chemistry and Physics Discussions

Table 3. Cross-model RMS differences (% of mean) for reactivities

P-O3	F0AM	GC	GISS	GMI	NCAR	UCI
F0AM		48%	95%	45%	55%	42%
GC	48%		78%	**26%**	42%	**32%**
GISS	95%	78%		81%	72%	74%
GMI	45%	**26%**	81%		40%	**35%**
NCAR	55%	42%	72%	40%		42%
UCI	42%	**32%**	74%	**35%**	42%	(10%)
L-O3						
F0AM		40%	44%	43%	76%	38%
GC	40%		33%	**25%**	60%	**24%**
GISS	44%	33%		36%	66%	30%
GMI	43%	**25%**	36%		62%	**28%**
NCAR	76%	60%	66%	62%		60%
UCI	38%	**24%**	30%	**28%**	60%	(11%)
L-CH4						
F0AM		47%	136%	48%	82%	45%
GC	47%		111%	**20%**	60%	**27%**
GISS	136%	111%		114%	110%	121%
GMI	48%	**20%**	114%		57%	**30%**
NCAR	82%	60%	110%	57%		68%
UCI	45%	**27%**	121%	**30%**	68%	(13%)

Calculated with the 31,376 MDS_R0 unweighted parcels that are a subset of the 32,383 MDS_R2 parcels. F0AM lacks 5,510 parcels because of the lack of observed J-values. UCI shows RMSD between years 2016 (default) and 1997 as the value in parentheses on diagonal. The unweighted mean from 3 core models (GC, GMI, UCI) are: P-O3 = 1.90, L-O3 = 1.24, L-CH4 = 0.51, all ppb/day.

619
620